Evaluation of Ruthenium Catalysts for Ring-Opening Metathesis Polymerization-Based Self-Healing Applications

Gerald O. Wilson,[†] Mary M. Caruso,[‡] Neil T. Reimer,[‡] Scott R. White,[§] Nancy R. Sottos,[†]
and Jeffrey S. Moore*,[‡]

*Beckman Institute and Departments of Materials Science and Engineering, Chemistry, and Aerospace
Engineering, University of Illinois at Urbana−Champaign, Urbana, Illinois 61801*

Received October 11, 2007. Revised Manuscript Received March 12, 2008

Self-healing polymers based on ring-opening metathesis polymerization incorporate first-generation Grubbs' catalyst as the polymerization initiator during a healing event. However, the use of this catalyst imposes limitations due to the catalyst's chemical and thermal instability typically encountered in processing and curing of epoxy resins. In this work, we compare three variations of Grubbs' catalysts (first generation, second generation, and Hoveyda−Grubbs' second generation) for use in self-healing polymers. Specifically, we examine the dissolution properties, initial polymerization kinetics, chemical stabilities, and thermal stabilities for all three catalysts. Furthermore, the reactivities of the three catalysts with various monomeric healing agents are compared with a view toward improving the self-healing performances in a variety of epoxy matrices, with disparate surface properties, by promoting noncovalent interactions between the epoxy matrices and the polymerized healing agents. Due to its thermal stability and functional group tolerance, second-generation Grubbs' catalyst emerges as the most versatile catalyst especially for high-temperature applications and use with healing chemistries aimed at improving self-healing performance via noncovalent interactions.

Introduction

Olefin metathesis is widely used for carbon−carbon bond-forming reactions in both organic and polymer chemistry.[1] The development of well-defined and stable ruthenium metathesis catalysts has increased the exploitation of olefin metathesis for the synthesis of small molecules, macromolecular architectures, and natural products in the presence of most common functional groups.[2] Our group has recently discovered another exciting application for these ruthenium catalysts, namely, in the development of ring-opening metathesis polymerization (ROMP)-based self-healing polymers.[3]

Two versions of ROMP-based self-healing polymers have been reported. In the first version, first-generation Grubbs' catalyst and urea−formaldehyde microcapsules containing dicyclopentadiene (DCPD) were embedded together in an epoxy matrix. Rupture of the microcapsules by a propagating crack releases DCPD into the crack plane where it contacts and reacts with the catalyst, initiating ROMP. The poly(D-CPD) formed in the crack plane bonds the crack and restores structural continuity.[3–6] In the second version, the Grubbs' catalyst was embedded in paraffin wax microspheres, which served the dual purpose of protecting the catalyst from deactivation by the diethylenetriamine (DETA) used to cure the epoxy and improving dispersion of the catalyst throughout the matrix. The use of catalyst microspheres resulted in a 90% decrease in the catalyst concentration required to achieve similar levels of healing efficiency compared to systems in which the catalyst phase was unprotected.[7,8]

The study of ROMP-based self-healing systems provides a general understanding of the requirements of an ideal self-healing polymer based on a one-capsule motif in which the healing agent (a monomer) is a microencapsulated liquid and the other component (a polymerization initiator) is embedded in the matrix as a solid. Characteristics of an ideal liquid healing agent include a long shelf life, prompt deliverability, high reactivity, and low volume shrinkage upon polymerization.[9] In addition, the liquid healing agent should not compromise the mechanical properties of the matrix in its encapsulated form, and the polymerized healing agent should exhibit exceptional intrinsic mechanical properties and good adhesion to the matrix. Ideal characteristics of the initiator

---

* To whom correspondence should be addressed. Fax: (217)-244-8024. E-mail: jsmoore@uiuc.edu.
  † Beckman Institute and Department of Materials Science and Engineering.
  ‡ Beckman Institute and Department of Chemistry.
  § Beckman Institute and Department of Aerospace Engineering.

 (1) Ivin, K. J.; Mol, J. C. *Olefin Metathesis and Metathesis Polymerization*; Academic Press: San Diego, CA, 1997.
 (2) Grubbs, R. H. *Handbook of Metathesis*; WILEY-VCH Verlag GmbH & Co. KGaA: Weinheim, 2003.
 (3) White, S. R.; Sottos, N. R.; Geubelle, P. H.; Moore, J. S.; Kessler, M. R.; Sriram, S. R.; Brown, E. N.; Viswanathan, S. *Nature* **2001,** *409,* 794–797.
 (4) Brown, E. N.; Sottos, N. R.; White, S. R. *Exp. Mech.* **2002,** *42,* 372–379.
 (5) Brown, E. N.; White, S. R.; Sottos, N. R. *Compos. Sci. Technol.* **2005,** *65,* 2474–2480.
 (6) Kessler, M. R.; Sottos, N. R.; White, S. R. *Composites: Part A* **2003,** *34,* 743–753.
 (7) Rule, J. D.; Brown, E. N.; Sottos, N. R.; White, S. R.; Moore, J. S. *Adv. Mater.* **2005,** *17,* 205–208.
 (8) Rule, J. D.; Sottos, N. R.; White, S. R. *Polymer* **2007,** *48,* 3520–3529.
 (9) Sriram, S. R. Ph.D. Thesis, University of Illinois at Urbana−Champaign, Urbana, IL; 2002.

include rapid dissolution in the liquid healing agent, fast initiation of polymerization, thermal stability at high processing and use temperatures, and chemical stability to matrix resins and curing agents. Together, these ideal characteristics represent a challenging list of requirements for the development of self-healing polymers with superior healing kinetics and high healing efficiencies.

In this paper, we compare three commercially available ruthenium catalysts with varying chemical, thermal, and catalytic properties. These catalysts include first-generation Grubbs' catalyst (**1**), which has been used with excellent results in a wide variety of self-healing applications;[3–8] second-generation Grubbs' catalyst (**2**), which has been reported to exhibit improved thermal stability and catalytic properties particularly in effecting metathesis of highly substituted and electron-poor olefins,[1,10–12] and Hoveyda–Grubbs' second-generation catalyst (**3**), which has demonstrated impressive chemical stability and recyclability.[13–15] Our evaluation of these catalysts specifically includes a comparison of their ROMP initiation kinetics, chemical stability to epoxy curing agents, thermal stability, and ROMP reactivity of alternative healing agents. Our aim is to expand the scope of the ROMP-based self-healing chemistry to more challenging application conditions.

Experimental Section

Catalysts **1**, **2**, and **3**, mesitylene, 5-norbornene-2-carboxylic acid (NCA, mixture of endo and exo), 5-ethylidene-2-norbornene (ENB), benzene-d_6, and methylene chloride-d_2 were obtained from Sigma-Aldrich and used as received from the supplier unless otherwise specified. Freeze-dried catalyst morphologies were obtained as reported elsewhere.[16] Dicyclopentadiene (DCPD) was obtained from Acros Organics and distilled and degassed (consecutive freeze−pump−thaw cycles) before use in kinetic experiments. For DCPD used in the preparation of self-healing polymer samples, 4-*tert*-butyl catechol (400 ppm) was added after distillation, prior to encapsulation. The resins EPON 828 and 862 were obtained from Miller-Stephenson Chemical Co., and the curing agents and additives, diethylenetriamine (DETA), Epicure 3274, Ancamine K54, and Heloxy 71 were obtained from Air Products and Chemicals Inc. All resins and curing agents were used as received unless otherwise specified. Environmental scanning electron microscopy (ESEM) images were taken using a Philips XL30 ESEM-FEG instrument using samples that had been sputter coated with gold−palladium. X-ray powder diffraction measurements were performed with a Bruker P4RA X-ray diffractometer using GADDS and a Cu Kα rotating anode equipped with a graphite monochromator. The beam width at the sample was approximately 0.6 mm. The powder sample was placed in a glass tube with thin walls (<0.1 mm). The scattering image of the empty tube was subtracted from the data.

Comparison of Solution ROMP Activity. ROMP activity for all three catalysts was compared by in situ NMR experiments performed on a Varian UNITY INOVA 500NB instrument. A solution of each catalyst (0.08 mM) in benzene-d_6 was prepared in an argon-filled glovebox, and 0.7 mL was transferred to an NMR tube. The tubes were then capped with septa and wrapped with parafilm. All solutions were used within a few hours of preparation. For each kinetic experiment, mesitylene (degassed by consecutive freeze−pump−thaw cycles, 10 μL) was added to the NMR tube prior to inserting the tube into the NMR instrument. The NMR sample was inserted into the instrument, and the probe temperature was brought to 25 °C. After thermal equilibration, the sample was removed and *endo*-DCPD (22.5 μL) was added by syringe. The sample was shaken and quickly reinserted into the instrument. Spectra were recorded every minute for 60 min with the sample left in the instrument at constant temperature for the duration of the experiment. DCPD concentration was monitored by comparing the resonance for the protons attached to the strained double bond (δ 5.90−6.02 ppm) to the signal from the ring protons on the mesitylene internal standard (δ 6.67 ppm).

Comparison of Bulk ROMP Activity. Bulk ROMP activity was evaluated by differential scanning calorimetry (DSC) experiments performed on a Mettler-Toledo DSC821ᵉ. Isothermal experiments (25 °C, 120 min) were performed for samples containing a mixture of DCPD and either catalyst **1** or **2** at a concentration of 3.6 mM (0.05 mol%). Monomer conversion (α_t) was determined as a function of time using eq 1

$$\alpha_t = 100\frac{Q_t}{Q_T} \tag{1}$$

where Q_t is the reaction heat at time t, as determined by integrating the isothermal heat (W/g) vs time (s) curve up to time t, and Q_T is an average of values for the heat of polymerization of DCPD initiated with catalyst **1** (468.4 J/g) using similar concentrations of catalyst that have been previously reported.[17] Similar experiments performed using catalyst **2** resulted in very similar values for the heat of polymerization of DCPD (see Supporting Information). To evaluate monomer conversion for samples containing **3**, the residual heat of polymerization measured by dynamic DSC (25−300 °C, 10 °C/min) was compared to the same average total heat of polymerization ($Q_T = 468.4$ J/g) as a function of time.

Dissolution Kinetics Measurements. The dissolution rates of the catalysts were measured in cyclohexane, which was qualitatively observed to dissolve the catalysts at rates similar to DCPD (but without polymerization). Four samples of approximately 5 mg of each catalyst were placed in separate unstirred vials with 3 mL of cyclohexane. At specified time intervals, each solution was filtered using 0.45 μm PTFE syringe filters and the concentration of catalyst in each solution was measured by UV−vis absorbance on a Shimadzu UV-2410PV spectrophotometer. The molar absorptivities for catalysts **1**, **2**, and **3** were measured to be 467 ($\lambda_{max} = 527$ nm), 404 ($\lambda_{max} = 504$ nm), and 160 M^{-1}cm^{-1} ($\lambda_{max} = 578$ nm), respectively.

Evaluation of Stability to DETA. The stability of the catalysts to DETA was evaluated by ^{1}H NMR on a UNITY 500 instrument. Stock solutions of each catalyst in methylene chloride-d_2 (0.24 mM) were prepared in an argon-filled glovebox, and 0.7 mL of each solution was added to separate NMR tubes. The tubes were capped with septa and sealed with parafilm. For each experiment, the NMR sample was inserted into the instrument and the probe temperature was brought to 25 °C. After acquisition of spectra for the initial

(10) Scholl, M.; Ding, S.; Lee, C. W.; Grubbs, R. H. *Org. Lett.* **1999**, *1*, 953–956.

(11) Bielawski, C. W.; Grubbs, R. H. *Angew. Chem., Int. Ed.* **2000**, *39*, 2903–2906.

(12) Huang, J.; Stevens, E. D.; Nolan, S. P.; Peterson, J. L. *J. Am. Chem. Soc.* **1999**, *121*, 2674–2678.

(13) Garber, S. B.; Kingsbury, J. S.; Gray, B. L.; Hoveyda, A. H. *J. Am. Chem. Soc.* **2000**, *122*, 8168–8179.

(14) Wakamatsu, H.; Blechert, S. *Angew. Chem., Int. Ed.* **2002**, *41*, 794–796.

(15) Bieniek, M.; Bujok, R.; Cabaj, M.; Lugan, N.; Lavigne, G.; Arit, D.; Grela, K. *J. Am. Chem. Soc.* **2006**, *128*, 13652–13653.

(16) Jones, A. S.; Rule, J. D.; Moore, J. S.; White, S. R.; Sottos, N. R. *Chem. Mater.* **2006**, *18*, 1312–1317.

(17) Kessler, M. R.; White, S. R. *J. Polym. Sci., Part A: Polym. Chem.* **2002**, *40*, 2373–2383.

Table 1. Matrix Preparation and Resulting Contact Angle Measurements

matrix designation	resin	additive [wt %]	curing agent [wt %]	H₂O contact angle (deg) [a]
M_1	EPON 828	N/A	DETA [10.7]	81[1]
M_2	EPON 828	HELOXY 71 [28.5]	Ancamine K54 [9.0]	82[3]
M_3	EPON 862	N/A	EPIKURE 3274 [33.3]	60[3]

[a] Standard deviation for contact angle measurements in square brackets.

a)

As-Received Catalyst Morphology

b)

Freeze-Dried Catalyst Morphology
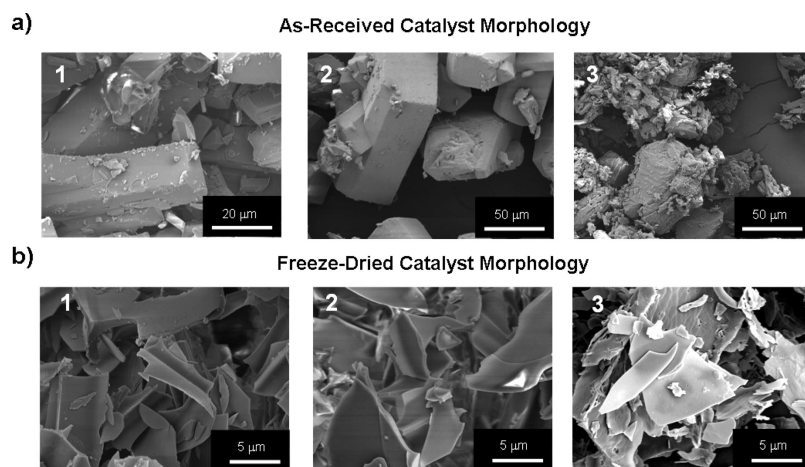
Figure 1. ESEM images comparing morphology of catalysts **1**–**3**: (a) as-received from Sigma-Aldrich and (b) obtained by freeze-drying.

catalyst solution, the tube was ejected and DETA (75 μL) was added. The tube was carefully shaken and quickly reinserted into the instrument. Spectra were recorded after 10 min in all cases and again after 4 h. The DETA used in these experiments was dried over CaH₂, distilled, and degassed (consecutive freeze−pump−thaw cycles) before use.

Contact Angle Measurements. Static contact angles were determined on epoxy surfaces using a Ramé-Hart model 100 Goniometer at room temperature (22 ± 1 °C). Contact angles were determined within 1 min of applying the water droplet to the surface. The tangent to the drop at its intersection with the surface was estimated visually. All reported values are the average of at least five measurements taken on each epoxy sample.

Fracture Specimen Preparation and Testing. All fracture specimens were prepared with a tapered double-cantilever beam (TDCB) geometry. The compositions for all epoxy matrices used in these tests are summarized in Table 1. Unless otherwise stated, all samples were cured at room temperature for 24 h followed by postcuring at 35 °C for 24 h. Testing followed an established procedure[4] in which a razor blade was used to initiate a precrack. The specimens were then pin loaded and tested under displacement control at a rate of 5 μm s⁻¹. Once completely fractured, the two halves of each specimen were brought back in contact and left to heal for 24 h at room temperature (unless otherwise noted) before retesting to failure.

Three types of fracture tests were performed. In reference tests, no healing agents were present in the matrix. Instead, the healing agent premixed with catalyst was injected into the crack plane after fracture, and the samples were left to heal for 24 h. In self-activated tests, the catalyst was embedded in the matrix, and the healing agent alone was injected into the crack plane at which point the samples were left to heal for 24 h. Finally, for in situ tests, catalyst and urea−formaldehyde microcapsules (average diameter of 250 ± 31 μm, prepared as reported elsewhere[18]) containing healing agent were embedded in the matrix. No healing agents were manually injected into the crack plane. For high-temperature experiments, the specimen was subjected to customary curing cycles,[3−7] followed by postcuring at 125 °C for 4 h before fracture testing. An average

retention of healing capacity (ρ_{avg}) based on a comparison of peak fracture loads of healed samples previously postcured at 125 °C to samples postcured at 35 °C is calculated according to eq 2.

$$\rho_{avg} = \frac{\mathrm{Avg}\left[P_c^{\ \mathrm{Healed}}\right]_{T_{postcure}=125°C}}{\mathrm{Avg}\left[P_c^{\ \mathrm{Healed}}\right]_{T_{postcure}=35°C}} \qquad (2)$$

Results and Discussion

Evaluation of Morphology and Dissolution Kinetics. Jones and co-workers observed that first-generation Grubbs' catalyst (**1**) can exist in several polymorphs.[16] Minor changes in processing conditions can lead to crystallization of different polymorphs.[19−21] Consequently, catalyst obtained from commercial sources exhibits different polymorphs even between different batches from the same supplier, making it difficult to design materials with reproducible properties. We successfully used a freeze-dry vacuum system with tunable pressure and temperature functions to generate high surface area first-generation Grubbs' catalyst morphologies reproducibly,[16] and this procedure was used without modification to generate freeze-dried morphologies for catalysts **2** and **3**.

As-received and freeze-dried morphologies for catalysts **1**−**3** were characterized by scanning electron microscopy (Figure 1) and X-ray powder diffraction (Figure 2). All catalysts in the as-received state exhibited very similar morphologies; particles were roughly 50−100 μm in length and 30 × 40 μm in cross section (Figure 1a). X-ray powder diffraction patterns for all three catalysts suggest that highly

(18) Brown, E. N.; Kessler, M. R.; Sottos, N. R.; White, S. R. *J. Microencapsulation* **2003**, *20*, 719–730.
(19) Hilker, R., Ed. *Polymorphism: in the Pharmaceutical Industry*; Wiley-VCH Verlag GmbH & Co.: Weinheim, 2006.
(20) Gardener, C. R.; Walsh, C. T.; Almarsson, O. *Nat. Rev. Drug Discov.* **2004**, *3*, 926–934.
(21) Mullin, J. B. *Crystallization*; Butterworth-Heinemann: Boston, MA, 2001.
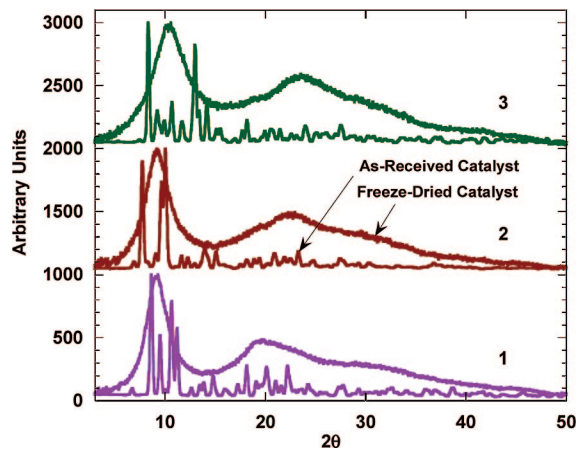
Figure 2. X-ray powder diffraction profiles comparing catalysts **1**−**3** in the morphology obtained from Sigma-Aldrich (lower trace in each pair) and the morphology obtained by freeze-drying (upper trace in each pair).
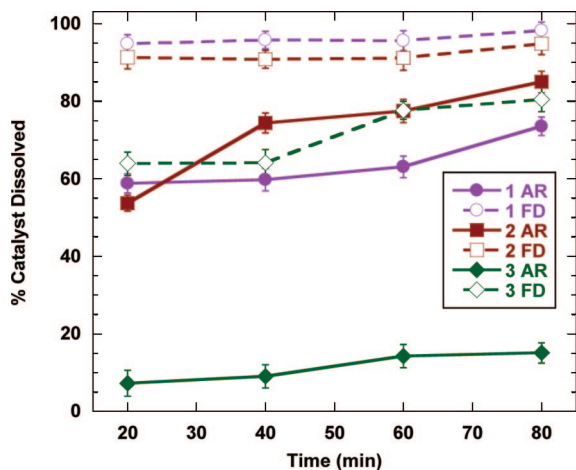
Figure 3. Comparison of dissolution rates in cyclohexane. AR designates as-received, and FD designates freeze-dried. Cyclohexane is used as a nonreactive mimic for DCPD.

crystalline solids are present (Figure 2). Freeze drying the catalysts resulted in the reproducible formation of amorphous polymorphs (Figure 2). ESEM images of the freeze-dried samples show a high surface area planar morphology of flakes, less than 1 μm thick. (Figure 1b). Freeze-dried samples of all three catalysts dissolved significantly faster in cyclohexane than as-received catalyst (Figure 3). For catalysts **1** and **2**, approximately 40% more catalyst dissolved within the first 20 min for freeze-dried samples compared to as-received samples. For catalyst **3**, approximately 50% more catalyst dissolved in the same period of time. However, catalyst **3** was observed to be intrinsically less soluble in cyclohexane with as much as 20% of the catalyst remaining undissolved after 80 min, even in the freeze-dried morphology.

Comparison of Initial ROMP Rates. Initial polymerization rates are of paramount importance in developing ROMP-based self-healing polymers since polymerization of healing agent released in the crack plane must occur before the monomer is lost by evaporation or absorption into the matrix. However, for optimal results polymerization initiation must not be so fast that it prevents dissolution of a sufficient amount of catalyst or impedes the transport of healing agent over the entire crack plane. A ^{1}H NMR comparison of the
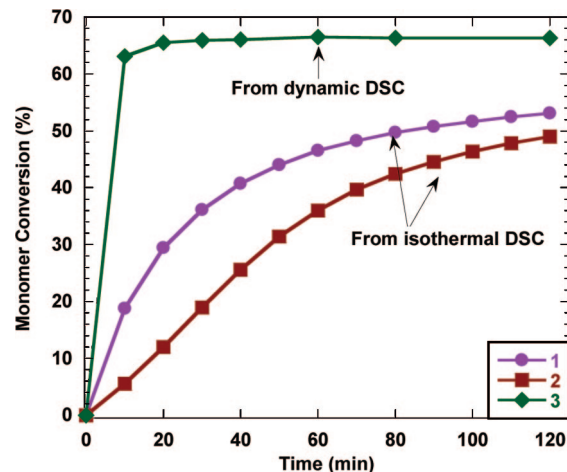
Figure 4. Comparison of initial kinetics of bulk ROMP of DCPD initiated by catalysts **1**−**3**. Monomer conversion was determined by differential scanning calorimetry (DSC). Monomer conversion in the presence of catalysts **1** and **2** was measured from isothermal experiments (25 °C), while monomer conversion for catalyst **3** was determined by measuring the residual heat of polymerization from dynamic experiments. Monomer conversion in the presence of all three catalysts was plotted on the same chart to facilitate direct comparison, although systematic differences are expected for measurements by these methods. Loading for all three catalysts was 3.6 mM (0.05 mol %).

ROMP of DCPD in solution (benzene-d_6) initiated by catalysts **1** and **2** yielded rate constants (k_{obs}) of 1.45×10^{-4} and 4.3×10^{-3} s^{-1}, respectively. The rate constants were determined using eq 3,[22,23] which is based on simpler kinetic behavior due to the establishment of a preequilibrium between the inactive five-coordinate form of the catalyst and the active four-coordinate form of the catalyst in the presence of added PCy$_3$ (see Supporting Information for kinetic plots).

$$-\frac{\text{d[monomer]}}{\text{d}t} = \frac{k[\text{Ru}]_0[\text{monomer}]}{[\text{PCy}_3]_0} \tag{3}$$

When a similar experiment was attempted with catalyst **3**, the DCPD polymerized instantaneously (too fast to measure) upon contact with the catalyst-containing solution. A similarly fast bulk polymerization of DCPD was observed with **3**, making it impossible to measure conversion isothermally (25 °C) by DSC, as was done for **1** and **2**. However, greater than 60% conversion of DCPD was observed after 10 min by measuring the residual heat of polymerization by dynamic DSC (Figure 4). Surprisingly and contrary to what was observed in solution, initial conversion of DCPD using **2** in bulk conditions was slower than conversion with **1** under the same conditions (Figure 4).

The increased ROMP activity observed in solution for catalyst **2** relative to **1** is consistent with observations of increased activity of **2** over **1** for metathesis of a variety of substrates.[10–12] It has been demonstrated that for solution-phase olefin metathesis reactions catalyzed by **1** and **2**, the first step of the reaction involves dissociation of the bound PCy$_3$ in the inactive 16-electron form of the catalyst to form

(22) Dias, E. L.; Nguyen, S. T.; Grubbs, R. H. *J. Am. Chem. Soc.* **1997**, *119*, 3887–3897.

(23) Sanford, M. S.; Ulman, M.; Grubbs, R. H. *J. Am. Chem. Soc.* **2001**, *123*, 749–750.

Scheme 1

Scheme 2

the active 14-electron intermediate.[23,24] This intermediate can be trapped by free PCy$_3$ to generate the starting inactive alkylidene or bind an olefin substrate and undergo metathesis (Scheme 1).[23] The activities of catalysts **1** and **2** therefore depend not only on phosphine dissociation but also on the ratio of the rate of phosphine reassociation (k_{-1}) and the rate of olefin binding (k_2). While phosphine dissociation occurs more rapidly in catalyst **1**, the ratio k_{-1}/k_2, which determines whether the 14-electron intermediate returns to the inactive 16-electron form or binds to the olefin, is significantly smaller for catalyst **2**.[23,24]

It is important to note that when a substrate contains more than one π-acidic olefin (as is the case with DCPD), both olefins are capable of binding to the ruthenium center after dissociation of the phosphine (Scheme 2). Whether the binding leads to a metathesis reaction or reassociation of the phosphine depends on the activation barriers that must be overcome. In the case of DCPD, the activation barrier for olefin association is probably lower for the strained norbornene olefin than it is for the cyclopentene olefin. As such, binding of the norbornene olefin will lead to metathesis more often than in the case of the cyclopentene olefin, which is less likely to react if at all. Furthermore, because catalyst **2** exhibits a greater preference for binding π-acidic olefins than **1**, in the ROMP of DCPD, k_{-N} and k_{-CP} (Scheme 2) can be expected to be smaller in the case of **2** than with **1**.

It is reasonable to extrapolate that in solution polymerization the solvent facilitates dissociation of both the phosphine (k_{-1}) and the olefin (k_{-2}) from the ruthenium center. However, in bulk polymerization where the monomer is the solvent, mass action favors binding of the olefin and disfavors olefin dissociation. A possible explanation for the depression of initial ROMP rates for polymerizations initiated with catalyst **2** relative to **1** could therefore involve the less likely dissociation of the cyclopentene olefin (smaller k_{-CP}) when bound to **2** versus **1** in bulk conditions. As such, initiation

(24) Sanford, M. S.; Love, J. A.; Grubbs, R. H. *J. Am. Chem. Soc.* **2001**, *123*, 6543–6554.

Figure 5. (a) TDCB geometry (dimensions in mm). (b) Example of a sample positioned in a load frame. The sample is precracked using a razor blade prior to positioning in the load frame. Uniaxial load is applied under displacement control at a rate of 5 μm s^{-1}. Self-healing materials were only included in the localized region.[8]

Figure 6. Effect of catalyst concentration on peak fracture load of self-activated healed samples. Monomer (10 μL) was injected into the crack plane, and samples were left to heal for 24 h at room temperature before retesting.

of the ROMP of DCPD by **2** is possibly attenuated by a greater affinity for the cyclopentene olefin relative to **1**. Elucidation of this difference in initial rates for ROMP of DCPD using **1** and **2** in bulk and solution conditions is the subject of ongoing research.

Chemical Compatibility with DETA. Much of our previous work has been based on the implementation of

Figure 7. Scanning electron microscopy (SEM) images of representative fracture planes for self-activated epoxy (M_1) samples containing 1.5 wt % as-received catalyst. Monomer (10 μL) was injected into the crack plane, and the samples were left to heal for 24 h before testing. A poly(DCPD) film is observed on the surface of the epoxy matrix, which is still visible underneath. The number labels on the images correspond to the catalyst used in the matrix.

ROMP self-healing chemistry in an epoxy matrix.[3–8,18,22] This matrix is comprised of the EPON 828 resin cured with DETA, which has been observed to deactivate the catalyst.[4,6,7] Paraffin wax has since been used to protect the catalyst from deactivation and improve its dispersion in the matrix.[7] However, the plasticization of poly(DCPD) formed in the crack plane during healing and the thermal instability of paraffin wax pose certain limitations on the applications in which ROMP-based self-healing polymers can be used.

The chemical compatibility of **1**−**3** with DETA was evaluated by measuring healing performance of an EPON 828/DETA matrix via self-activated fracture tests. This matrix is designated M_1 in Table 1. To prepare these samples, a specified amount of each catalyst was stirred into a degassed mixture of the EPON 828 and DETA prior to casting the resin in a silicone mold with the TDCB geometry (Figure 5). The samples were then allowed to cure at RT (approximately 25 °C) for 24 h followed by postcuring at 35 °C for 24 h. After precracking and loading to failure, DCPD (10 μL)[25] was carefully injected into the crack plane. Polymerization of the healing agent was activated by catalyst exposed on the fracture plane, and the samples were then allowed to heal for 24 h at RT before retesting.

The first set of experiments was performed using as-received catalyst since this more robust morphology (Figure 1a) was expected to be more capable of resisting deactivation by DETA. The effect of catalyst concentration on the peak fracture loads of healed samples is summarized in Figure 6. The results obtained with **1** are consistent with observations made by Brown and co-workers[4] in which healing efficiency was observed to increase with catalyst concentration. In this work, the peak fracture load of the healed sample was observed to increase monotonically as the catalyst concentration was varied from 0.5 to 2.5 wt %. The catalyst maintained its dark purple color in the matrix. Peak fracture loads of healed samples containing **2** and **3** begin to plateau at a catalyst concentration of 1.5 wt %. ESEM images of representative samples containing 1.5 wt % of catalysts **1**−**3** (Figure 7) show good coverage of the fracture planes in all three cases. Lower average peak fracture loads observed for **2** and **3** compared to **1** at higher concentrations of catalyst can be attributed to a lower degree of cure throughout the poly(DCPD) film formed on the fracture plane. In the case of **2**, lower peak fracture loads at higher concentrations are likely due to lower initial bulk ROMP rates. On the other hand, excessively rapid polymerization rates and poor dissolution of **3** in DCPD presumably result in inefficient

Table 2. Summary of Self-Activated and in Situ Tests for Epoxy (EPON® 828 cured with DETA, M_1) Samples Containing the Three Types of Catalysts in the Freeze-Dried Morphology

catalyst	type of test[a,b]	no. of samples	peak fracture load of healed sample (N)
1	self-activated	5	0
2	self-activated	4	32.1[3.4]
3	self-activated	4	20.2[4.7]
1	in situ	5	0
2	in situ	4	28.1[2.9]
3	in situ	4	19.8[5.3]

[a] Self-activated samples contain 2.5 wt % catalyst only. [b] In-situ samples contain 2.5 wt % catalyst and 10 wt % microcapsules.

use of catalyst and hence a lower degree of cure[17] than is required for good mechanical properties.

Self-activated healing tests were also performed for samples from all three catalysts in their freeze-dried morphologies. Due to the susceptibility of high surface area morphologies to deactivation,[16] only the largest concentration of catalyst (2.5 wt %) was evaluated. Upon adding **1** to the curing mixture of the EPON 828 resin and DETA (M_1 matrix), the purple catalyst turned brown immediately. This color change is indicative of deactivation of the catalyst.[4,9] A color change (from brown to green) was also observed for catalyst **2**, while no obvious color change was observed for **3**. The self-activated test results for freeze-dried catalysts are summarized in Table 2. No healing was observed with catalyst **1**, while average peak fracture loads of healed samples containing **2** and **3** were 32.1 ± 3.4 and 20.2 ± 4.7 N, respectively. A similar observation was made for in situ tests in which the samples contained 2.5 wt % of a specific catalyst and 10 wt % of DCPD microcapsules (250 ± 31 μm). Again, healing was observed with **2** and **3** but not with **1** (Table 2). An evaluation of the respective fracture planes (Figure 8) shows ruptured microcapsules in samples containing **1**, indicating that DCPD had been released into the fracture plane, but no poly(DCPD) was observed, while poly(DCPD) films were observed for samples containing **2** and **3**.

The effect of DETA on catalysts **1**−**3** was also evaluated by a series of NMR experiments. DETA (50 μL) was added by syringe to solutions of each catalyst in methylene chloride-d_2 (0.24 mM). ^{1}H NMR spectra taken after 10 min showed formation of new carbene resonances for all three catalysts.

(25) In earlier work on self-healing materials, Brown and co-workers[4] injected 30 μL of DCPD into the crack plane of self-activated samples. Rule et al.[8] have since demonstrated that injecting 10 μL results in a more accurate correlation with in situ results.
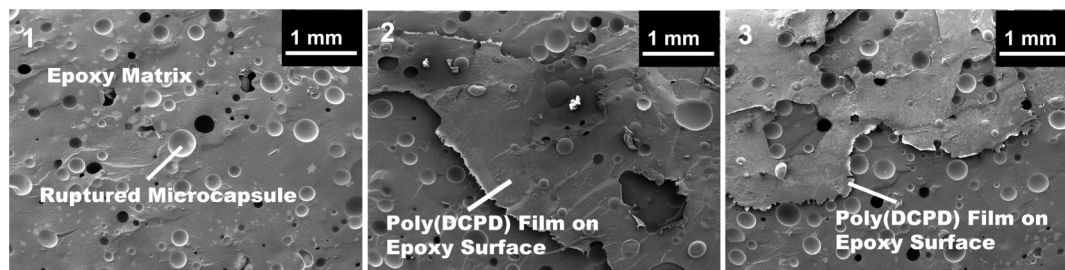
Figure 8. Scanning electron microscopy (SEM) images of representative fracture planes for in situ epoxy (M_1) samples containing 2.5 wt % freeze-dried catalyst and 10 wt % microcapsules (average diameter = 250 ± 32 mm). After fracture, the samples were left to heal for 24 h before testing. In the case of catalyst **1**, ruptured microcapsules are observed in the epoxy matrix, while for catalysts **2** and **3**, a poly(DCPD) film is observed on the surface of the epoxy matrix which is still visible underneath. The number labels on the images correspond to the catalyst used in the matrix.

In the case of **1**, the intensity of this new resonance (δ 19.3 ppm) was much weaker and continued to diminish. The new carbene resonances observed for **2** (δ 19.0 ppm) and **3** (δ 19.3 ppm) were of a much higher intensity and persisted beyond the first 10 min, with that of **2** appearing to be the most stable by being the only resonance still present in the carbene region up to 2 h. Phosphorus NMR (^{31}P NMR) spectra were also taken for **1** and **2** under otherwise identical conditions. For **1**, free tricyclohexylphosphine (PCy_3) was the predominant species detected along with several other smaller unidentifiable phosphine signals that appeared after addition of DETA. For **2**, free PCy_3 was the only phosphine signal observed under identical conditions. Formation of new relatively stable carbenes in the case of **2** and **3** is consistent with isolation of ruthenium complexes in which the phosphine ligand was replaced by pyridine[26] and bromopyridine.[27] The transient formation of a new carbene when DETA was added to the solution of **1** in methylene chloride-d_2 suggests formation of an unstable bis-DETA ruthenium complex that presumably undergoes decomposition via a bimolecular mechanism.[28,29] Ongoing work is focused on further elucidation of the apparently greater ability of ruthenium catalysts containing N-heterocyclic ligands to stabilize new complexes with primary amines.

While the self-healing performance of samples containing **2** and **3** does not improve on existing systems employing **1**,[4,18] reproducible freeze-dried morphologies of **2**, in particular, form new catalytically active ruthenium complexes in situ that can be exploited for self-healing applications.

Thermal Stability of Catalysts. The thermal decomposition of derivatives of Grubbs' catalyst in solution has been extensively studied.[29] In self-healing applications however the catalyst is embedded into the polymer matrix as a solid and the activity of the catalyst over the lifetime of the material depends on its stability to processing conditions during manufacture and environmental conditions during use. For application of ROMP-based self-healing chemistry in matrices that are often exposed to high-temperature curing conditions or high use temperature, the thermal stability of catalysts in the solid phase was evaluated. DSC

Table 3. Summary of Healing Performance for Epoxy (M_1) Samples Containing 1.5 wt % Catalyst, Postcured at 125 °C and Healed at RT or 125 °C, in Comparison To Samples Postcured at 35°C and Healed at RT^a

catalyst	no. of samples	healing temperature (°C)	peak fracture load (N) of healed sample	retention of healing capacity (ρ_{avg}, %)
none	3	RT	0	N/A
1	3	RT	23.1[3.5]	77
2	3	RT	22.4[6.0]	84
3	4	RT	5.3[2.1]	18
none	3	125	0	N/A
1	3	125	32.8[12.1]	109
2	4	125	57.6[13.3]	216
3	3	125	16.7[6.0]	57

^{a} Control samples contained no catalyst and showed no healing.

experiments in air and N_2 confirmed that thermal stability is higher for as-received catalyst morphology versus freeze dried, and the former was used for evaluation of high-temperature applications.

To evaluate the thermal stability of the catalysts under simulated high-temperature processing conditions self-activated M_1 samples containing 1.5 wt % of as-received catalyst were prepared and subjected to customary curing cycles[3–7] followed by an additional postcuring at 125 °C for 4 h. Samples were then fractured, and DCPD (10 μL) was injected into the crack plane. The samples were then left to heal at either RT or 125 °C for 24 h. Compared to the self-activated samples postcured at 35 °C (Figure 6) and healed at RT, retention of healing performance for RT healing was 77%, 84%, and 18% for **1**, **2**, and **3**, respectively (Table 3). Samples healed at 125 °C showed significant improvements over those healed at RT, with the highest average peak fracture load of 57.6 ± 13.6 N obtained for samples containing **2**. Representative load-displacement curves (Figure 9) show that in addition to the increased peak fracture load observed for samples containing **1** and **2** (healed at 125 °C), these samples exhibit more brittle failure indicative of a higher degree of cure of the poly(DCPD) formed in the crack plane. An increase in peak fracture load is observed for similarly cured and healed samples containing **3**, but this increase is smaller (18%) than for samples containing **1** and **2**, and ductile failure is still observed. This result suggests a lack of sufficient catalyst dissolved in the healing agent to promote a higher degree of cure at elevated temperature. Furthermore, highly essential to good self-healing performance is the ability of the healing agent to adequately wet

(26) Sanford, M. S.; Love, J. A.; Grubbs, R. H. *Organometallics* **2001**, *20*, 5314–5318.
(27) Love, J. A.; Morgan, J. P.; Trnka, T. M.; Grubbs, R. H. *Angew. Chem., Int. Ed.* **2002**, *41*, 4035–4037.
(28) Dias, E. L.; Grubbs, R. H. *Organometallics* **1998**, *17*, 2758–2767.
(29) Ulman, M.; Grubbs, R. H. *J. Org. Chem.* **1999**, *64*, 7202–7207.
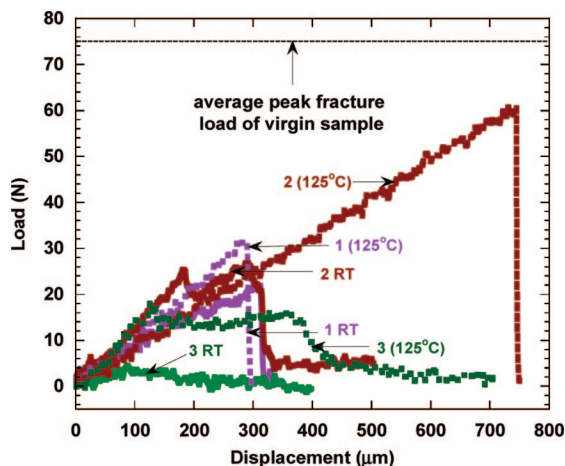
Figure 9. Representative load-displacement curves for self-activated epoxy (M_1) samples containing 1.5 wt % of catalyst **1**, **2**, or **3** (labeled accordingly), postcured at 125 °C and healed at room temperature or 125 °C.

the crack plane during a healing event.[16] Moreover, the initial ROMP rates may be too fast at these temperatures for that to occur.

Evaluation of the Potential of Alternative Healing Agents. In current self-healing systems[3–7] the healing efficiency depends on the combination of adhesive and cohesive failure mechanisms of the healed sample. Improving the healing efficiency requires improving adhesion of the polymer formed in the crack plane to the matrix without compromising the mechanical properties associated with the cohesive strength of poly(DCPD). Polymer additives commonly referred to as compatibilizers have been used to reinforce the interfaces between immiscible polymers.[30,31] In this section, we evaluate a similar approach to improving the healing efficiency of ROMP-based self-healing polymers.

Three different epoxy matrices (Table 1, Chart 1) were selected for this study. The first matrix (M_1) was EPON 828 cured with DETA, which has been used thus far in this study and in a variety of ROMP-based self-healing polymers.[3–8] The remaining two matrices, EPON 828 containing Heloxy 71 as a flexibilizer and cured with Ancamine K54 (M_2) and EPON 862 cured with EPICURE 3274 (M_3), have been evaluated as possible matrices for new self-healing polymers.[32–34]

5-Norbornene-2-carboxylic acid (NCA, Chart 2) was evaluated as an adhesion promoter since it contains a norbornene functional group capable of copolymerization with DCPD and a carboxylic acid functional group for hydrogen bonding with amine and hydroxyl functional groups in epoxy resins. Healing performance was evaluated by fracture of neat resin TDCB samples followed by manual injection of healing agent premixed with catalyst and 24 h healing time at RT. The healing agents injected were DCPD,

(30) Kramer, E. J.; Norton, L. J.; Dai, C. A.; Sha, Y.; Hui, C. Y. *Faraday Discuss.* **1994**, *98*, 31–46.
(31) Sha, Y.; Hui, C. Y.; Kramer, E. J.; Hahn, S. F.; Berglund, C. A. *Macromolecules* **1996**, *29*, 4728–4736.
(32) Kessler, M. R.; White, S. R. *Composites: Part A* **2001**, *32*, 683–699.
(33) Brown, E. N. Ph.D. Thesis, University of Illinois at Urbana-Champaign, Urbana, IL, 2003.
(34) Patel, A. J.; Sottos, N. R.; White, S. R. *Proceedings of the First International Conference on Self Healing Materials*, Noordwijk, The Netherlands, April 18–20, 2007.

Chart 1

Chart 2
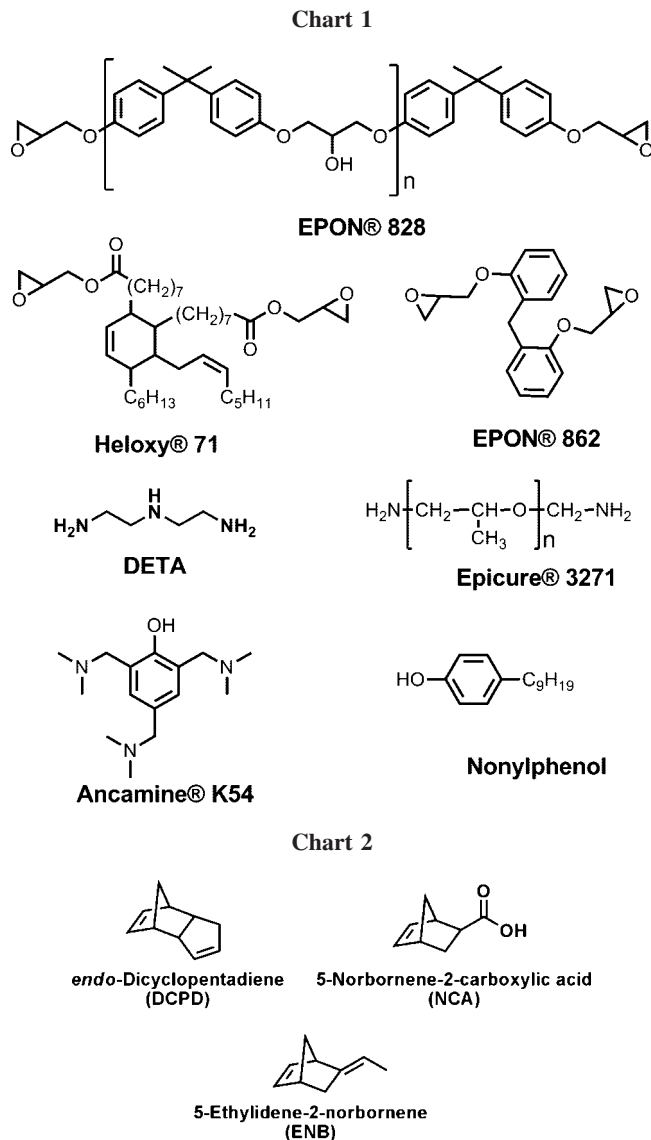
a DCPD/NCA blend, and a DCPD/5-ethylidene-2-norbornene (ENB) blend, all containing 5 mg/mL of catalyst **2**. ENB served as a control healing agent additive to ensure that any improvements observed by addition of NCA was not due to
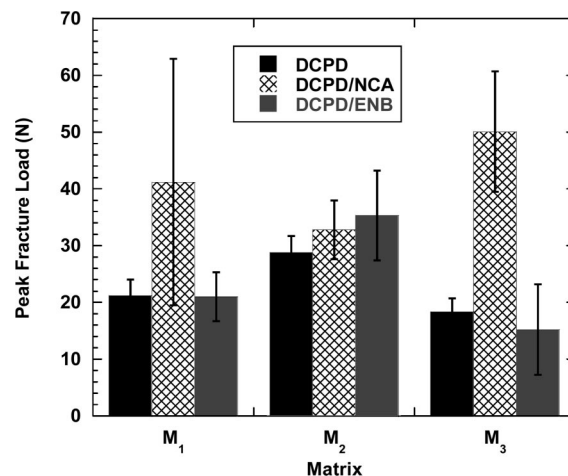
Figure 10. Average peak fracture loads of M_1, M_2, and M_3 samples healed with DCPD, DCPD/NCA, and DCPD/ENB. Each column is an average of data for 3–4 samples, and the error bars represent one standard deviation.
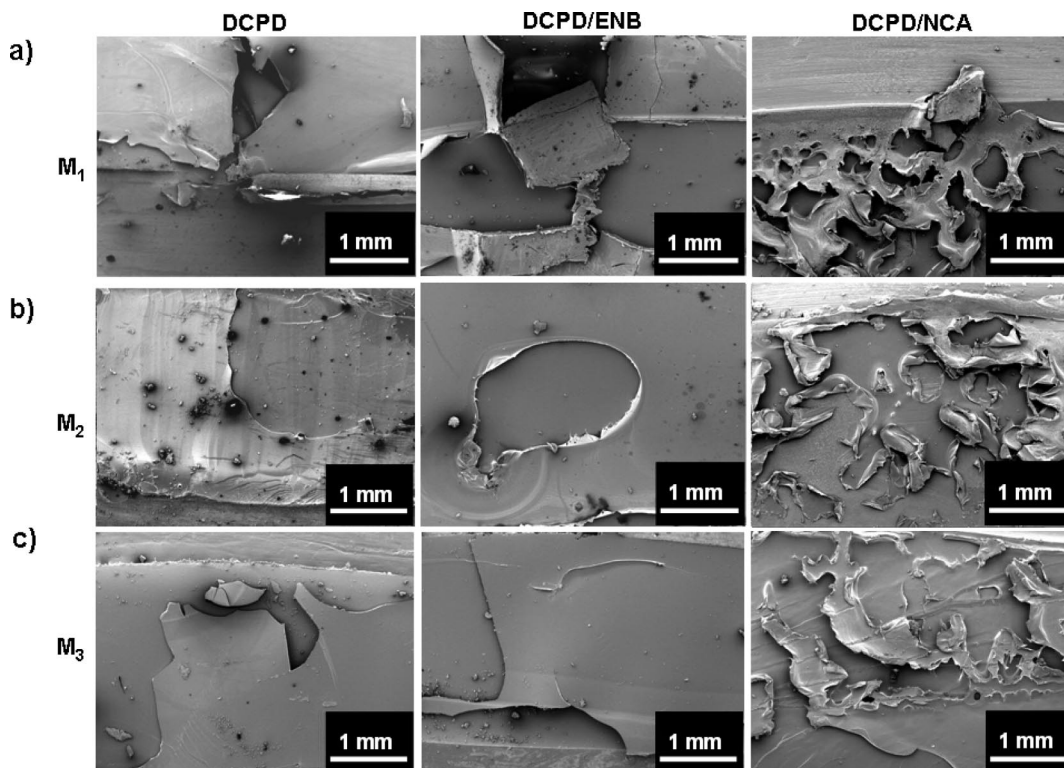
Figure 11. Representative fracture planes for samples healed with DCPD, DCPD/ENB, and DCPD/NCA from left to right on M_1 (a), M_2 (b), and M_3 (c). Polymerized healing agent is observed as a film on the surface of the matrix (M_1–M_3), which is still visible underneath.

faster initial ROMP rates of the potentially less sterically hindered norbornene olefin in NCA relative to DCPD or more facile chain entanglement as a result of lower cross-link density in the DCPD copolymer relative to the homopolymer. The results of these experiments are summarized in Figure 10. For all reference tests in which **2** was the catalyst used, the highest peak fracture load (50.05 ± 10.62 N) was observed for M_3 (which had the smallest H_2O contact angle of 60 ± 3°) healed with the DCPD/NCA blend. The use of the DCPD/NCA blend also led to higher peak fracture loads for healed M_1 and M_2 samples. Matrix M_2 (H_2O contact angle 82 ± 3°) had the smallest difference in performance between the various healing agents. These results suggest that the healing efficiency can be improved by carefully matching matrices with healing agents to maximize noncovalent interactions. While all healing agent blends were consistently polymerized by **2**, peak fracture loads for samples healed with a mixture of the DCPD/NCA blend and **1** were consistently zero as **1** was incapable of initiating polymerization when the carboxylic acid group was present. Catalyst **3** was also qualitatively observed to polymerize all healing agent blends, but polymerization was too fast for injection of these mixtures into the crack plane of the reference test samples. Examination of representative fracture planes for all three matrices, each healed with three varieties of healing agent (Figure 11), shows that failure of samples healed with DCPD and the DCPD/ENB blend is mainly adhesive as large unbroken films of poly(DCPD) or the DCPD/ENB copolymer remain intact on one-half of the TDCB sample. In contrast and consistent with more cohesive failure, all samples healed with the DCPD/NCA blend show

ruptured and discontinuous DCPD/NCA copolymer films on one-half of the sample.

Conclusion

Catalysts **2** and **3** exhibited significantly improved initial polymerization rates relative to **1**. However, faster initial solution ROMP rates for DCPD did not result in improved self-healing performance since in the case of **2** corresponding bulk ROMP rates did not improve relative to catalyst **1**. For **3**, initial bulk ROMP rates were significantly faster than the corresponding dissolution rates, but this resulted in self-limiting polymerization and inefficient use of catalyst. Recrystallization of catalysts **1**–**3** by freeze drying resulted in formation of high surface area amorphous solids with improved dissolution properties. However, freeze-dried catalysts were more susceptible to the chemical incompatibilities of DETA, which included deactivation of **1** and formation of new metathesis active complexes in situ with **2** and **3**. Catalyst **2** exhibited the best thermal stability in self-activated healing tests and readily polymerized a mixture of DCPD and NCA, which showed improved performance as a healing agent in EPON 828 and 862 resins. In general, catalysts **1**–**3** exhibited different dissolution properties, thermal and chemical stabilities, and functional group tolerance which can be exploited for self-healing polymers with more finely tuned properties for specific applications.

Supporting Information Available: Comparison of initial solution ROMP kinetics for DCPD with catalysts **1** and **2**, dynamic DSC curves for ROMP of DCPD with catalyst **2** and corresponding determination of the heat of polymerization, figures comparing the colors of epoxy matrices containing as-received catalyst and freeze-dried catalyst, NMR data showing the effect of DETA on the catalysts, and comparison of thermal stability of the catalysts by TGA and DSC (PDF). This material is available free of charge via the Internet at http://pubs.acs.org.

CM702933H